Journal of Ceramic Processing Research. Vol. 14, No. 4, pp. 459~462 (2013)

J O U R N A L O F
Ceramic Processing Research

Synthesis and photo-catalysis properties of ZnO micro-flowers by precipitation method

J. Moghaddam[a,]* and S. Mollaesmail[a]

[a]*Materials and Metallurgical Engineering Department, Advanced Materials Research Center, Sahand University of Technology, P.O. Box: 51335-1996, Tabriz, Iran*

ZnO micro-flowers were successfully synthesized by precipitation method via an ammonical ammonium carbonate zinc aqueous solution in presence of oleic acid. Oleic acid as additive could affect on morphology and photo-catalysis properties of ZnO particles. The structure and morphology of products were characterized by X-ray diffraction (XRD), Scanning electron microscopy (SEM), UV- visible spectroscopy, Raman spectroscopy and Photoluminescence (PL) analysis. ZnO with flower like morphology exhibited improved ability on the photo-catalytic degradation of Methyl Blue (MB) dye wastewater compared with sphere like nano particles under UV radiation. The higher photo-catalytic activity of the ZnO micro-flowers result from the larger content of oxygen vacancy on the surface of nano-materials as revealed by their Raman and Photoluminescence (PL) spectra features.

Key words: ZnO, Nano-structured, Photo-catalysis, Precipitation method.

Introduction

The photo-catalytic degradation of organic pollutants in water and air, using semiconductors such as TiO_2 and ZnO have attracted more attention due to its incomparable ability in the environment oxidization. The advantage of photo-catalytic process is that it works at ambient conditions of temperature and pressure without forming any kind of sludge, which otherwise creates another pollution problem [1-5].

In recent years, many researchers have reported that ZnO powders have a more powerful photo-catalytic reaction rather than TiO_2, because ZnO powders can absorb larger fraction of the solar spectrum than TiO_2 powders can. It is evident that the desired photo-catalytic activity strongly related to the particle sizes and shapes of ZnO powders. For this reason, many researchers have focused on the synthesis of different morphologies of ZnO powders due to the fact that they displayed the unique properties [6-7].

It has been found that ZnO can be synthesized by various routes such as pulsed laser deposition [8], sono-chemical [9], gel combustion method [10] and precipitation [11] methods. Among these methods, precipitation has many advantages over the other methods, for example, it is unsophisticated and a low cost method.

Until now, one dimensional ZnO nanostructures such as wires, rods and tubes, and two-dimensional structures including sheets and ribbon shave been synthesized [12, 13]. In addition, the three-dimensional ZnO complex structures built up through the low-dimensional components, for example, rings, bows, helices, springs and interconnected nanowire networks, have received increasing attention recently [14-18].

In this study, ZnO micro-flowers and spherical nano-particles were synthesized via an ammonical ammonium carbonate zinc aqueous solution in two conditions (e.g. without and presence of oleic acid as additive). Moreover, the photo-catalytic activity of these powders was characterized by measuring degradation of methyl blue (MB) as a function of time.

Materials and Methods

Materials

ZnO powders were synthesized according pervious work that based on super-saturation theory [19]. Because of achieving nano-scale particles production from precipitation method, so it needs a homogeneous nucleation from a super-saturation solution. Primary tests showed that the maximum solubility and most practical condition were achieved at pH = 9.5 and T = 85 °C. First of all, 500 ml of 2 M ammonium carbonate solution was placed into the beaker. When the beakers content reached its desired temperature (85 °C), ammonia was slowly added to adjust pH (9.5). The value of pH was determined by a digital pH-meter (Inolab, model listed 8F93). Zinc oxide was added into the solutions until to reach the saturated solution. In this stage, oleic acid as additive added into the main solution to produce ZnO micro-flowers. The point of

*Corresponding author:
Tel : +98-412-3443802
Fax: +98-412-3443443
E-mail: moghaddam@sut.ac.ir; hastyir@yahoo.com (J. Moghaddam)

cloud formation and precipitation were investigated for 150 min. After this time, the precipitates were filtered, rinsed by deionized water, dried at 105 °C for 24 hr and finally calcinated at 400 °C for 1 hr.

Characterization

The structure of as-prepared samples was determined by the use of X-ray diffraction (XRD, Philips with Cu-Kα radiation). The morphology of particles was studied by scanning electron microscope (SEM, Philips XL30). The Raman spectroscopy was conducted with Reinishaw model 3000 in the range of 200-800 cm^1. The photoluminescence (PL) spectra were recorded on a Varian Cary-Eclipse spectrometer at the range of 440 to 600 nm.

Measurement of the photo-catalytic properties

The morphology-dependent photo-catalytic activities of the as-prepared ZnO particles were evaluated by degradation of MB dye wastewater under UV light irradiation. All the experiments were done at temperature 25 ± 2 °C. Two UV lamps that predominantly emit at 365 nm with the definite power 150 W were employed as the light source. They were positioned parallel to the 500 mL Pyrex glass bottle that was used to load the dye solutions in the photo-catalytic process. The distance between the top of Pyrex glass bottle and the UV lamp was 10 cm. The photo-catalytic experiments were carried out with 200 mL dyes solutions, which were sonicated for 15 min and stirred in the dark for 20 min after the addition of (0.05 gr) ZnO photo-catalysts. Finally, the concentration of MB dye was measured as a function of time with a UV-Vis spectrophotometer (UV-Vis 2550, Shimadzu).

Results and Discussion

Structure and morphology

XRD patterns of the ZnO micro-flowers (A) and spherical nano-particles (B) are shown in Fig. 1. All of the diffraction peaks in the patterns can be exactly indexed as the hexagonal wurtzite ZnO with lattice constants a = 0.3249 nm and c = 0.5206 nm, which are agreed well with the values in the standard card (JCPDS 36-1451). No characteristic peaks were observed for the other impurities. In addition, all peaks of ZnO micro-flowers (A) much higher and narrower shaped than spherical shape ZnO (B), which indicates that formers have good crystallite quality than spherical shape one.

Figure 2 shows SEM images of ZnO powders that synthesized in two different conditions. According Figure 2(a), the obtained ZnO powders without any additive have a spherical shape. These powders resulted from the calcinations at a temperature of 400 °C for 1 h. The morphology of the powders synthesized in presence of Oleic acid as additive (Fig. 2(b)) showed ZnO flower-like micro-particles. The cause of this phenomenon is effect of Oleic acid on the growth of ZnO particles. By adding Oleic acid, ZnO nuclei grow along c direction because these points were energetically favored to adsorb zinc on the outer surfaces. Those nuclei at early stage act as seeds for growing of the ZnO precursor along the preferred growth direction. After completing synthesis, ZnO precursor grows along different directions and micro-flowers are formed [20].

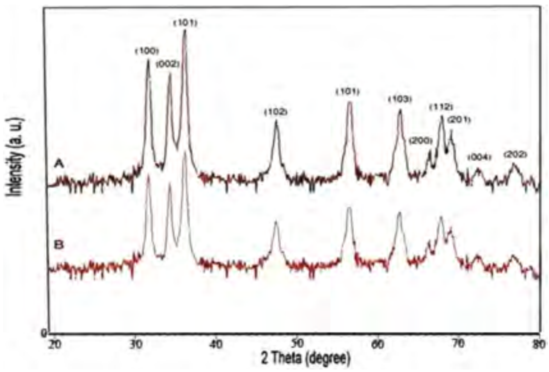

Fig. 1. XRD patterns of the as-prepared samples, (A) ZnO micro flowers and (B) spherical ZnO nano-particles.

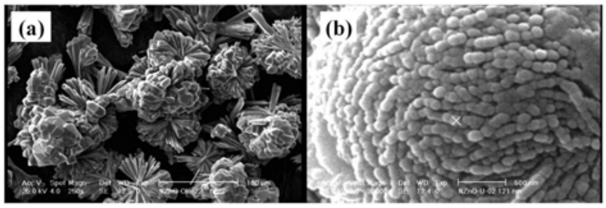

Fig. 2. SEM image of the ZnO micro-flowers (a) and spherical ZnO (b).

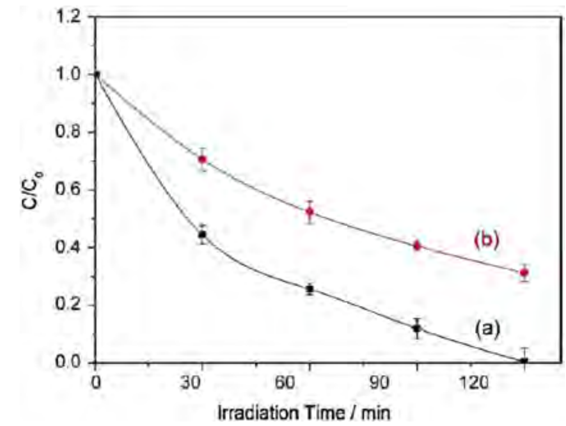

Fig. 3. Process of photo-catalytic degradation of MB dye wastewater under UV light illumination over two photo-catalysts: (a) ZnO micro-flowers, (b) Spherical ZnO.

Photo-catalytic activity

As illustrated in Fig. 3, the photo-catalytic activities of ZnO micro-flowers and spherical one were investigated on the photo-degradation of MB dye wastewater under UV light irradiation. One can see clearly from Fig. 3 that the photo-degradation of MB dye wastewater is

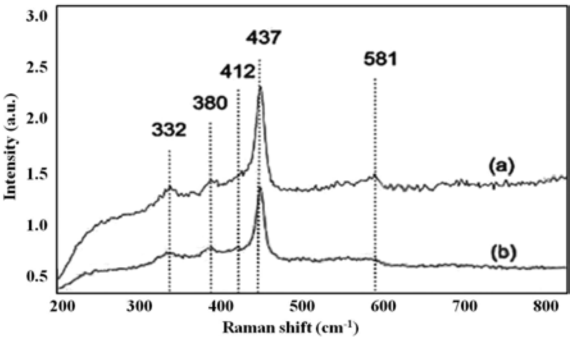

Fig. 4. Raman spectra of the as-prepared ZnO: (a) flower-like morphology and (b) spherical ZnO.

more efficient by ZnO micro-flowers (Fig. 3a) than by ZnO spherical shape (Fig. 3b). The MB dye wastewater in aqueous solutions can be almost completely eliminated by ZnO micro-flowers while spherical ZnO show 80% degradation of MB dye wastewater after illuminated by UV light for 120 min. It is essential to understand the mechanism of semiconductor photo-catalysis. It is generally accepted that, when semiconductor nano-crystals are irradiated by light with higher or equal to the band gap energy, an electron (e^-) in the valence band (V_B) can be excited to the conduction band (C_B) with the simultaneous generation of a hole (h^+) in the V_B.

The higher photo-catalytic activity of the ZnO micro-flowers may result the larger content of oxygen vacancy on the surface. The photo-electron can be easily trapped by electronic acceptors like adsorbed O_2, to further produce a superoxide radical anion (O_2^-), whereas the photo-induced holes can be easily trapped by electronic donors, such as organic pollutants, to further oxidize organic pollutants. However, if the photo-generated electrons recombined with the photo-induced holes, the photo-catalytic activity would be decreased. In general, oxygen vacancy of defect in ZnO crystallinity can act as the active centers to capture photo-induced electrons, and the recombination of photo-induced electrons and holes can be effectively inhibited, so that the photo-catalytic activity can be greatly improved [21, 22].

Raman and PL analyses of the as-prepared ZnO micro-flowers and spherical ZnO are performed to examine their defects. The Raman spectra of the ZnO micro-flowers and spherical ZnO at the range of 200-800 cm^1 are shown in Fig. 4. The dominant feature at 437 cm^1 is the result of ZnO non-polar optical phonons E_2 (high) mode. The E_2 (high) mode corresponds to characteristic band of hexagonal wurtzite phase. The peak located at 332 cm^1 may be attributed to a multi-phonon scattering process (E_{2H}-E_{2L}) [23]. The peaks at 380 and 412 cm^1 correspond to A_1 (TO) and E_1 (TO) phonons of ZnO crystal, respectively. In addition, the E_1 (LO) peak can also be observed at 581 cm^1. The appearance of the E_1 (LO) peak is associated with the formation of defects such as oxygen vacancy, zinc interstitial, or their complexes [24]. It can be seen that the E_1 (LO) peak of the ZnO micro-flowers (see Fig. 4a) is stronger than that of the spherical ZnO (see Fig. 4b).

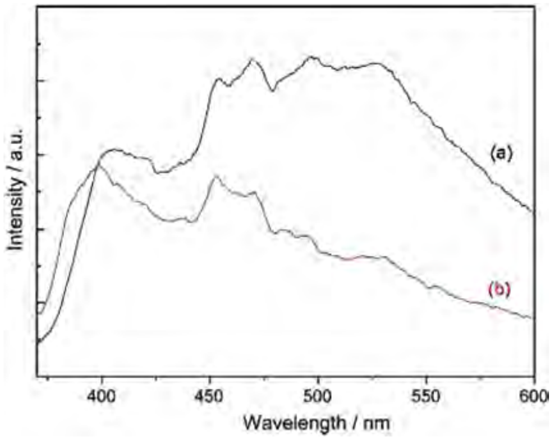

Fig. 5. PL spectra of the as-prepared ZnO: (a) flower-like morphology and (b) spherical ZnO.

PL spectra of the as-prepared ZnO micro-flowers and spherical ones are shown in Fig. 5. Each PL spectrum possesses a common feature that consists of an ultraviolet (UV) peak and a visible emission band. Generally, the UV peak is due to the recombination of photo-generated electrons and holes, while the visible emission ranging from 440 to 600 nm is associated with oxygen vacancies [25]. In this work, the visible emission of ZnO micro-flowers is much stronger than spherical ones, suggesting that the content of oxygen vacancy in ZnO micro-flowers is more than spherical ones. Based on the above results, it can be concluded that more defects exist in the ZnO micro-flowers, which causes higher photo-catalytic activity than ZnO particles with spherical shapes. Therefore, the difference in photocatalytic activities for different morphology of ZnO samples is mainly caused by oxygen vacancy, which can act as active centers.

Conclusions

In summary, micro-flower ZnO have been successfully synthesized via an ammonical ammonium carbonate zinc aqueous solution via precipitation method in presence of oleic acid as additive. The results showed that ZnO micro-flowers have the higher photo-catalytic activity than spherical ones for degradation of MB dye wastewater under UV light irradiation. Raman and PL spectra analyses indicates that the as-prepared ZnO samples all have oxygen vacancy, and the oxygen vacancy content of ZnO micro-flowers is more than the spherical one.

References

1. B. Swarnalata, Y. Anjaneyulu, J. Mol, Catal. A: Chem. 223 (2004) 161-165.

2. C.C. Chen, J. Mol, Catal. A: Chem. 264 (2007) 82-92.
3. Ch. Chen, B. Yu, P. Liu, J.F. Liu and L. Wang, J. Ceram. Process. Res. 12 (2011) 420-425.
4. M.J. Height, S.E. Pratsinis, O. Mekasuwandumrong, P. Praserthdam, Appl. Catal. B: Environ. 63 (2006) 305-312.
5. S.K. Pardeshi, A.B. Patil, Sol. Energy 82 (2008) 700-705.
6. R.Y. Hong, J.H. Li, L.L. Chen, D.Q. Liu, H.Z. Li, Y. Zheng, J. Ding, Powder Technol. 189 (2009) 426-432.
7. G. Mahmoudzadeh, S.A. Khorrami, S.S. Madani and M. Frounchi, J. Ceram. Process. Res. 13 (2012) 368-372.
8. H.W. Lee, B.G. Choi, K.B. Shim and Y.J. Oh, 6 (2005) 52-56.
9. P. Mishra, R.S. Yadav, A.C. Pandey, Ultrason. Sonochem. 17 (2010) 560-565.
10. N. Riahi-Noori, R. Sarraf-Mamoory, P. Alizadeh and A. Mehdikhani, J. Ceram. Process. Res. 9 (2008) 426-249
11. N. Samaele, P. Amornpitoksuk, S. Suwanboon, Mater. Lett. 64 (2010) 500-502.
12. S.J. Chen, Y.C. Liu, C.L. Shao, R. Mu, Y.M. Lu, J.Y. Zhang, D.Z. Shen, X.W. Fan, Adv. Mater. 17 (2005) 586-590.
13. M.S. Wang, E.J. Kim, E.W. Shin, J.S. Chung, S.H. Hahn, C. Park, J. Phys. Chem. C 112 (2008) 1920-1924.
14. B. Liu, S.H. Yu, F. Zhang, L.J. Li, Q. Zhang, L. Ren, K. Jiang, J. Phys. Chem. B 108 (2004) 4338-4341.
15. W.L. Hughes, Z.L. Wang, Appl. Phys. Lett. 86 (2005) 043106-1-043106-3.
16. P.X. Gao, Y. Ding, W.J. Mai, W.L. Hughes, C.S. Lao, Z.L. Wang, Science 309 (2005) 1700-1704.
17. P.X. Gao, Z.L. Wang, Small. 1 (2005) 945-949.
18. P.X. Gao, C.S. Lao, W.L. Hughes, Z.L. Wang, Chem. Phys. Lett. 408 (2005) 174-178.
19. Javad Moghaddam, Seyed Behnam Ghaffari, Rasoul Sarraf-Mamoory, and Sara Mollaesmail, Synth. React. Inorg. Me. in press.
20. Feifei Wang, Li Cao, Anlian Pan, Ruibin Liu, Xiao Wang,Xing Zhu, Shiquan Wang, and Bingsuo Zou, J. Phys. Chem. C 111 (2007) 7655-7660.
21. L.Q. Jing, Y.C. Qu, B.Q. Wang, S.D. Li, B.J. Jiang, L.B. Yang, W. Fu, H.G. Fu, J.Z. Sun, Sol. Energy Mater. Sol. Cells 90 (2006) 1773-1787.
22. X.P. Lin, T. Huang, F.Q. Huang, W.D. Wang, J.L. Shi, J. Phys. Chem. B 110 (2006) 24629-24634.
23. T.C. Damen, S.P.S. Porto, B. Tell, Phys. Rev. 142 (1966) 570-574.
24. A.K. Pradhan, K. Zhang, G.B. Loutts, U.N. Roy, Y. Cui, A. Burger, J. Phys.: Condens. Matter 16 (2004) 7123-7129.
25. K. Vanheusden, W.L. Warren, C.H. Seager, D.R. Tallant, J.A. Voigt, B.E. Gnade, J. Appl. Phys. 79 (1996) 7983-7990.